

Specific heat and effects of pairing fluctuations in the BCS-BEC-crossover regime of an ultracold Fermi gas

Pieter van Wyk, Hiroyuki Tajima, Ryo Hanai, and Yoji Ohashi

Department of Physics, Keio University, 3-14-1 Hiyoshi, Kohoku-ku, Yokohama 223-8522, Japan

(Received 24 September 2015; published 25 January 2016)

We investigate the specific heat at constant volume C_V in the Bardeen-Cooper-Schrieffer–Bose-Einstein-condensate (BCS-BEC)-crossover regime of an ultracold Fermi gas above the superfluid phase transition temperature T_c . Within the framework of the strong-coupling theory developed by Nozières and Schmitt-Rink, we show that this thermodynamic quantity is sensitive to the stability of preformed Cooper pairs. That is, while $C_V(T \gtrsim T_c)$ in the unitary regime is remarkably enhanced by *metastable* preformed Cooper pairs or pairing fluctuations, it is well described by that of an ideal Bose gas of long-lived *stable* molecules in the strong-coupling BEC regime. Using these results, we identify the region where the system may be viewed as an almost ideal Bose gas of stable pairs, as well as the pseudogap regime where the system is dominated by metastable preformed Cooper pairs, in the phase diagram of an ultracold Fermi gas with respect to the strength of a pairing interaction and the temperature. We also show that the calculated specific heat agrees with the recent experiment on a ${}^6\text{Li}$ unitary Fermi gas. Since the formation of preformed Cooper pairs is a crucial key in the BCS-BEC-crossover phenomenon, our results would be helpful in considering how fluctuating preformed Cooper pairs appear in a Fermi gas to eventually become stable as one passes through the BCS-BEC-crossover region.

DOI: [10.1103/PhysRevA.93.013621](https://doi.org/10.1103/PhysRevA.93.013621)

I. INTRODUCTION

The formation of preformed Cooper pairs is a crucial key in considering the Bardeen-Cooper-Schrieffer–Bose-Einstein-condensate (BCS-BEC)-crossover phenomenon [1–11], where the character of a Fermi superfluid continuously changes from the weak-coupling BCS type to the BEC of tightly bound molecules with increasing of the strength of a pairing interaction. Since the realization of this crossover phenomenon in ${}^{40}\text{K}$ [12] and ${}^6\text{Li}$ [13–15] Fermi gases by using a Feshbach resonance [16–18], it has extensively been discussed both theoretically [19–29] and experimentally [30–42] how metastable preformed Cooper pairs (that are also referred to in the literature as pairing fluctuations) appear in a Fermi gas to eventually become long-lived stable pairs as one passes through the BCS-BEC-crossover region above the superfluid phase transition temperature T_c . Since the BCS-BEC-crossover is also considered as a crucial key in the fields of high- T_c cuprates [10,43], as well as iron based superconductors [44], elucidating strong-coupling properties of an ultracold Fermi gas in this regime would also contribute to the understanding of these strongly correlated electron systems.

Although there is no clear phase boundary between the weak-coupling BCS regime and the strong-coupling BEC regime, it is still an interesting problem to physically identify the region where preformed Cooper pairs dominate over system properties. In this regard, we note that when preformed Cooper pairs appear in a normal Fermi gas, single-particle Fermi excitations are expected to have a gaplike structure, reflecting their finite dissociation energy. This so-called preformed pair scenario has been discussed in high- T_c cuprates [45] as a possible mechanism of the pseudogapped density of states observed in the underdoped regime of this strongly correlated electron system [46–49]. In this field, the temperature T^* below which the pseudogap appears in the density of states $\rho(\omega)$ is called the pseudogap temperature.

Although T^* is not accompanied by any phase transition, it is a useful characteristic temperature to distinguish between the normal Fermi liquid regime and the pseudogap regime in the phase diagram of high- T_c cuprates.

In high- T_c cuprates, the validity of the preformed pair scenario is still in debate [45,50–52] due to the complexity of this system. In contrast, since an ultracold Fermi gas in the BCS-BEC-crossover region is simply dominated by strong pairing fluctuations, the preformed pair scenario is validated. Indeed, it has been pointed out [26,36] that the back-bending curve of the single-particle dispersion observed by a recent photoemission-type experiment on a ${}^{40}\text{K}$ unitary Fermi gas [34] may be a signature of the pseudogap phenomenon. It has also been shown [27,29] that the anomalous suppression of the uniform spin susceptibility χ_s observed in a ${}^6\text{Li}$ Fermi gas above T_c [40] can be explained as an effect of fluctuating spin-singlet preformed pairs. At present, although the pseudogap temperature T^* has not experimentally been determined in an ultracold Fermi gas, the existence of this characteristic temperature has theoretically been predicted from the calculated density of states $\rho(\omega)$ [24]. As in the case of high- T_c cuprates, T^* in an ultracold Fermi gas is not accompanied by any phase transition. However, it physically gives the boundary between a normal Fermi gas regime and the pseudogap regime, being dominated by fluctuating preformed Cooper pairs, in the phase diagram of an ultracold Fermi gas above T_c .

A similar characteristic temperature T_s , called the spin-gap temperature, has also been predicted [29]. T_s is determined as the temperature below which the spin susceptibility χ_s in the normal state is anomalously suppressed by spin-singlet preformed Cooper pairs. Although T_s is not exactly the same as the pseudogap temperature T^* , they have essentially the same background physics, and thus T_s also has the meaning of the boundary between the normal Fermi gas regime and the preformed-pair regime. We briefly note that this so-called

spin-gap phenomenon [53] has also been discussed in high- T_c cuprates [54,55].

Although T^* and T_s conveniently give the boundary around which metastable preformed Cooper pairs start to dominate over the system in the BCS-BEC-crossover region, they do not have any information about where these fluctuating preformed pairs become stable in the strong-coupling BEC regime. In determining this second boundary, however, the low-energy density of states $\rho(\omega \sim 0)$ (which gives the pseudogap temperature T^*), as well as the spin susceptibility χ_s (which gives the spin gap temperature T_s), are not useful, because both quantities almost vanish deep inside the BEC regime where most Fermi atoms form spin-singlet bound molecules with a large binding energy.

In this regard, the specific heat at constant volume C_V is promising, because it is finite in the whole BCS-BEC-crossover region. In addition, C_V is sensitive to the quantum statistics of particles in the system in the sense that, while C_V exhibits a linear-temperature dependence in a Fermi gas, it increases with decreasing of the temperature in an ideal Bose gas. Furthermore, the specific heat has recently become accessible in cold Fermi gas physics [41]. Thus, the above-mentioned second boundary may be determined by using this thermodynamic quantity.

The purpose of this paper is to theoretically confirm this expectation, to distinguish between the pseudogap regime, which is dominated by metastable preformed Cooper pairs or pairing fluctuations, and the region that can be viewed as a gas of long-lived stable pairs in the phase diagram of an ultracold Fermi gas. Including pairing fluctuations above T_c within the framework of the strong-coupling theory developed by Nozières and Schmitt-Rink [3], we show that the temperature dependence of the specific heat is very different in between the BCS-BEC-crossover region and the strong-coupling BEC regime. Using this difference, we determine a characteristic temperature \tilde{T} which conveniently gives the boundary between the pseudogap regime and the region of stable pairs. In addition, the specific heat is also shown to be able to determine the boundary between the normal Fermi gas regime and the pseudogap regime. The characteristic temperature \tilde{T} giving the latter boundary is found to be consistent with the previous pseudogap temperature T^* , as well as the spin-gap temperature T_s , that are, respectively, obtained from the density of states $\rho(\omega)$ and the spin susceptibility χ_s . We also show that our result on C_V agrees with the recent experiment on a ^6Li unitary Fermi gas [41]. We briefly note that the specific heat in a unitary Fermi gas has also been discussed within a T -matrix approximation [39], as well as within the combined NSR theory with local density approximation [20].

This paper is organized as follows. In Sec. II, we explain our strong coupling formalism used to calculate the specific heat at constant volume C_V in the BCS-BEC-crossover region above T_c . In Sec. III, we show our numerical results on C_V over the entire BCS-BEC-crossover region. Here, we explain how to determine \tilde{T} and \bar{T} from the temperature dependence of C_V . Using these characteristic temperatures, we identify the region where the system is dominated by fluctuating metastable preformed Cooper pairs, as well as the region where the system is dominated by long-lived stable molecules, in the phase diagram of an ultracold Fermi gas with respect to

the interaction strength and the temperature. Throughout this paper, we set $\hbar = k_B = 1$, and the system volume V is taken to be unity for simplicity.

II. FORMULATION

We consider a two-component uniform Fermi gas in the normal state, described by the BCS Hamiltonian,

$$H = \sum_{p,\sigma} \xi_p c_{p,\sigma}^\dagger c_{p,\sigma} - U \sum_{p,p',q} c_{p+q/2,\uparrow}^\dagger c_{-p+q/2,\downarrow}^\dagger c_{-p'+q/2,\downarrow} c_{p'+q/2,\uparrow}, \quad (1)$$

where $c_{p,\sigma}$ is the annihilation operator of a Fermi atom with pseudospin $\sigma = \uparrow, \downarrow$, describing two atomic hyperfine states. $\xi_p = \varepsilon_p - \mu = \mathbf{p}^2/(2m) - \mu$ is the kinetic energy, measured from the Fermi chemical potential μ (where m is an atomic mass). $-U$ is an s -wave pairing interaction, which we treat as a tunable parameter. As usual, we measure the interaction strength in terms of the s -wave scattering length a_s , which is related to the pairing interaction $-U$ as

$$\frac{4\pi a_s}{m} = -\frac{U}{1 - U \sum_p^{p_c} \frac{1}{2\varepsilon_p}}, \quad (2)$$

where p_c is a momentum cutoff.

We include pairing fluctuations within the ordinary NSR theory [3]. In this BCS-BEC-crossover theory, the thermodynamic potential $\Omega = \Omega_0 + \Omega_{\text{NSR}}$ consists of the noninteracting part,

$$\Omega_0 = -2T \sum_p \ln[1 + e^{-\xi_p/T}], \quad (3)$$

and the fluctuation correction Ω_{NSR} , the latter of which is diagrammatically given in Fig. 1. The summation of these diagrams gives

$$\Omega_{\text{NSR}} = -T \sum_{q,i\nu_n} \ln \Gamma(\mathbf{q}, i\nu_n), \quad (4)$$

where ν_n is the boson Matsubara frequency, and

$$\Gamma(\mathbf{q}, i\nu_n) = \frac{1}{\frac{m}{4\pi a_s} + \left[\Pi(\mathbf{q}, i\nu_n) - \sum_p \frac{1}{2\varepsilon_p} \right]} \quad (5)$$

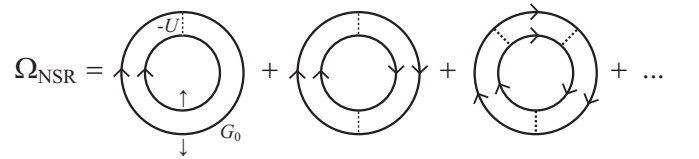


FIG. 1. Feynman diagrams describing the correction term Ω_{NSR} to the thermodynamic potential Ω in the strong-coupling NSR theory [3]. The solid line is the bare single-particle thermal Green's function $G_0^{-1}(\mathbf{p}, i\omega_n) = i\omega_n - \xi_p$ (where ω_n is the fermion Matsubara frequency), and the dashed line is the attractive pairing interaction $-U$.

is the NSR particle-particle scattering matrix. Here,

$$\Pi(\mathbf{q}, i\nu_n) = - \sum_p \frac{1 - f(\xi_{p+q/2}) - f(\xi_{-p+q/2})}{i\nu_n - \xi_{p+q/2} - \xi_{-p+q/2}} \quad (6)$$

is the lowest-order pair-correlation function, describing fluctuations in the Cooper channel [where $f(x)$ is the Fermi distribution function].

We calculate the specific heat at constant volume C_V from the formula

$$C_V = \left(\frac{\partial E}{\partial T} \right)_{V,N}. \quad (7)$$

Here, the internal energy E is obtained from $\Omega = \Omega_0 + \Omega_{\text{NSR}}$ via the Legendre transformation,

$$\begin{aligned} E &= \Omega - T \left(\frac{\partial \Omega}{\partial T} \right)_\mu - \mu \left(\frac{\partial \Omega}{\partial \mu} \right)_T \\ &= 2 \sum_p \varepsilon_p f(\xi_p) - T \sum_{\mathbf{q}, i\nu_n} \Gamma(\mathbf{q}, i\nu_n) \\ &\quad \times \left[T \frac{\partial}{\partial T} \Pi(\mathbf{p}, i\nu_n) + \mu \frac{\partial}{\partial \mu} \Pi(\mathbf{q}, i\nu_n) \right]. \end{aligned} \quad (8)$$

The Fermi chemical potential μ in Eq. (8) is determined from the equation for the total number N of Fermi atoms, given by

$$\begin{aligned} N &= - \left(\frac{\partial \Omega}{\partial \mu} \right)_T \\ &= 2 \sum_p f(\xi_p) - T \sum_{\mathbf{q}, i\nu_n} \Gamma(\mathbf{q}, i\nu_n) \frac{\partial}{\partial \mu} \Pi(\mathbf{q}, i\nu_n) \\ &= N_F^0 + N_{\text{NSR}}, \end{aligned} \quad (9)$$

where N_F^0 and N_{NSR} represent the noninteracting part and the NSR strong-coupling corrections, respectively. In this paper, we numerically evaluate Eq. (7) from the internal energies $E(T)$ and $E(T + \delta T)$.

In the NSR theory [3–6], the equation for the superfluid phase transition temperature T_c is conveniently obtained from the Thouless criterion [56], stating that the superfluid instability occurs when the particle-particle scattering matrix $\Gamma(\mathbf{q}, i\nu_n)$ in Eq. (5) has a pole at $\mathbf{q} = \nu_n = 0$. The resulting T_c equation has the same form as the mean-field BCS gap equation at T_c , as

$$1 = - \frac{4\pi a_s}{m} \sum_p \left[\frac{1}{\xi_p} \tanh \frac{\xi_p}{2T} - \frac{1}{2\varepsilon_p} \right]. \quad (10)$$

Following the standard NSR approach [3–6], we numerically solve the T_c equation (10), together with the number equation (9), to self-consistently determine T_c and $\mu(T_c)$ in the BCS-BEC-crossover region. Above T_c , we only deal with the number equation (9) to determine $\mu(T)$, which is used to evaluate the specific heat C_V .

III. SPECIFIC HEAT IN THE BCS-BEC-CROSSOVER REGION ABOVE T_c

Figure 2(a) shows the specific heat at constant volume C_V in the BCS-BEC-crossover regime of an ultracold Fermi gas at $T = T_c$. As expected, C_V in the weak-coupling BCS regime

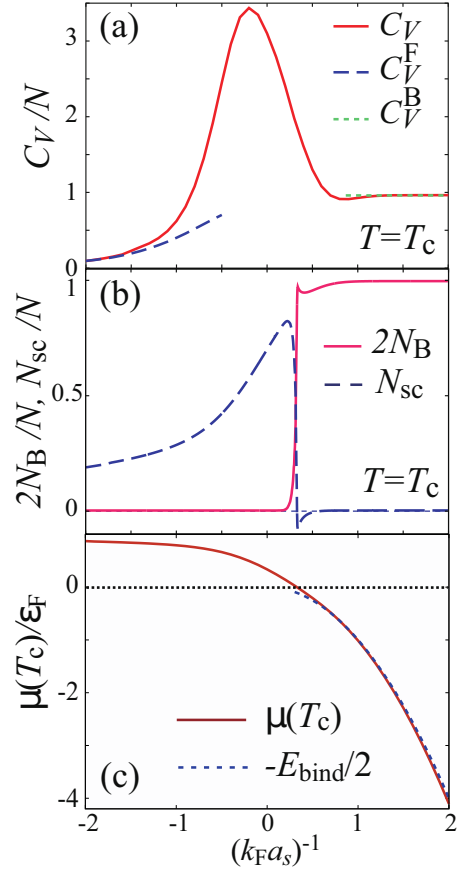


FIG. 2. (a) Calculated specific heat C_V at T_c , as a function of the interaction strength measured in terms of the inverse scattering length $(k_F a_s)^{-1}$, normalized by the Fermi momentum k_F . We also plot the specific heat $C_V^F(T = T_c)$ in a free Fermi gas, as well as the specific heat C_V^B in Eq. (12). (b) The number of stable molecules N_B at T_c . N_{sc} is the contribution from scattering states at T_c . (c) Fermi chemical potential $\mu(T = T_c)$, normalized by the Fermi energy ε_F . The dashed line shows $-E_{\text{bind}}^2/2$, where $E_{\text{bind}} = 1/(ma_s^2)$ is the binding energy of a two-body bound molecule.

$[(k_F a_s)^{-1} \lesssim -1]$, where k_F is the Fermi momentum], as well as that in the strong-coupling BEC regime $[(k_F a_s)^{-1} \gtrsim 1]$ are, respectively, well described by the specific heat in a free Fermi gas [57],

$$C_V^F(T \ll T_F) = \frac{\pi^2}{2} \left(\frac{T}{T_F} \right) N \quad (11)$$

(where T_F is the Fermi temperature), and the specific heat in an ideal Bose gas with $N/2$ molecules at the BEC phase transition temperature $T_{\text{BEC}} = 0.218 T_F$ [3–5, 58],

$$C_V^B(T = T_{\text{BEC}}) = \frac{15}{4} N_B \frac{\zeta(5/2)}{\zeta(3/2)} = 0.963 N, \quad (12)$$

where $\zeta(3/2) = 2.612$ and $\zeta(5/2) = 1.341$ are zeta functions. Although C_V continuously changes from C_V^F to C_V^B in the BCS-BEC crossover, it experiences anomalous enhancement in the unitary regime $[(k_F a_s)^{-1} \sim 0]$, as seen in Fig. 2(a).

This remarkable enhancement of C_V originates from the suppression of the entropy $S = \ln W$ by the appearance of preformed Cooper pairs near T_c . Since the number of possible

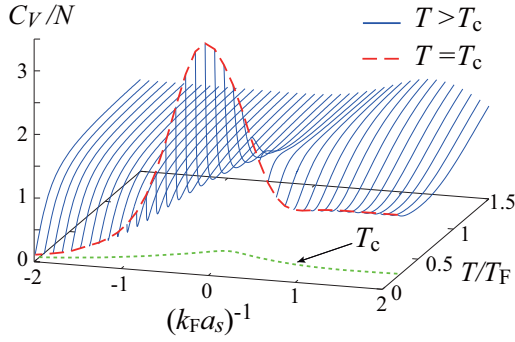


FIG. 3. Calculated specific heat C_V , as a function of the temperature in the BCS-BEC-crossover regime of an ultracold Fermi gas above T_c . The dashed line shows the result at T_c .

microstates W in a gas of bound molecules with nearly zero center of mass momentum is smaller than W in a simple unbound Fermi gas, the gradual formation of preformed Cooper pairs with decreasing temperature nearing T_c suppresses the entropy S . When this suppression is more remarkable at lower temperatures, the thermodynamic formula,

$$C_V = T \left(\frac{\partial S}{\partial T} \right)_{V,N}, \quad (13)$$

immediately gives the enhancement of C_V . In the unitary regime, such preformed-pair formation occurs near T_c , so that the amplification of C_V is also restricted to the region near T_c , as shown in Fig. 3.

To see whether these preformed Cooper pairs are stable or fluctuating, it is convenient to divide the NSR correction term N_{NSR} in the number equation (9) into the sum of twice the number N_B of *stable* molecules and the so-called scattering part N_{sc} [3] involving a contribution from fluctuating *metastable* preformed pairs [6,59]. The resulting expression for the total number N of Fermi atoms has the form

$$N = N_F^0 + 2N_B + N_{\text{sc}}. \quad (14)$$

(For detailed expressions for N_B and N_{sc} , see the Appendix.) Then we find in Fig. 2(b) that there are no *stable* preformed pairs ($N_B = 0$) in the unitary regime where C_V is remarkably amplified [60], which means that this enhancement is due to the increase of *metastable* preformed Cooper pairs or pairing fluctuations.

Figure 2(b) also indicates that the strong-coupling BEC regime [$(k_F a_s)^{-1} \gtrsim 0.3$] is dominated by long-lived *stable* molecules ($N_B \simeq N/2$). This naturally explains why $C_V(T = T_c)$ in this regime is well described by C_V^B in Eq. (12). As shown in Fig. 2(c), this result is also consistent with the well-known result for the Fermi chemical potential μ in that it becomes negative in the BEC regime, and the magnitude $|\mu|$ approaches half the binding energy $E_{\text{bind}}^{2b} = 1/(ma_s^2)$ of a two-body bound state in the strong-coupling limit [3–6,59].

As seen in Fig. 3, the amplification of C_V in the unitary regime near T_c disappears as one moves to the BEC side [$(k_F a_s)^{-1} \gtrsim 0$]. To see this more clearly, we summarize in Fig. 4 the temperature dependence of C_V slightly in the BEC side. Noting that long-lived *stable* molecules appear when $(k_F a_s)^{-1} \gtrsim 0.3$ [see Fig. 2(b)], we expect that the thermal

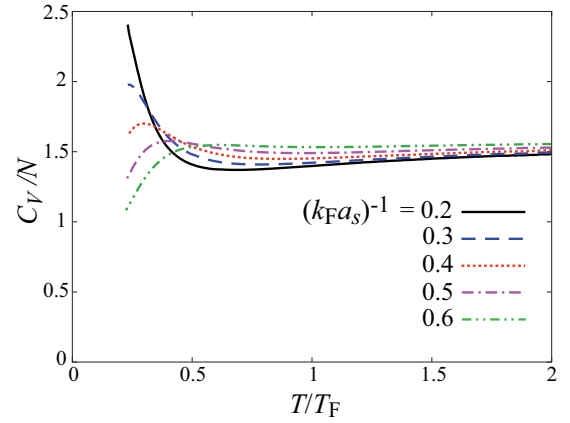


FIG. 4. Specific heat C_V in the BEC side, $0.2 \leq (k_F a_s)^{-1} \leq 0.6$.

dissociation of these molecules (with a relatively small binding energy E_{bind}) is responsible for the temperature dependence of C_V near T_c in this regime. Indeed, simply taking into account this effect by dealing with a two-level system with energy $\omega = 0$ and $\omega = E_{\text{bind}}$, one has

$$C_V = \left(\frac{E_{\text{bind}}}{2T} \right)^2 \text{sech}^2 \left(\frac{E_{\text{bind}}}{2T} \right), \quad (15)$$

which monotonically increases with increasing of the temperature when $T \lesssim E_{\text{bind}}/2$. This is just the behavior of $C_V(T \gtrsim T_c)$ shown in Fig. 4 when $(k_F a_s)^{-1} \gtrsim 0.3$, indicating that the increase of C_V with increasing of the temperature near T_c in this region originates from the thermal dissociation of *stable* molecules.

We note that the key to understanding the reason why the temperature dependence of C_V near T_c slightly in the BEC regime is qualitatively different from that in the unitary regime is the stability of preformed pairs. In the former BEC case where long-lived *stable* molecules ($N_B \simeq N/2$) with a finite binding energy E_{bind} dominate over the system, thermal dissociation of molecules leads to exponential-like temperature dependence of various thermodynamic quantities. Because of this, the entropy S becomes a *concave* function of temperature, so that the specific heat C_V given by Eq. (13) becomes an increasing function of the temperature. On the other hand, in the case of unitary regime with no *stable* molecule ($N_B = 0$), because *metastable* preformed Cooper pairs are actually pairing fluctuations where formation and dissociation of preformed pairs repeatedly and frequently occur, the binding energy of such a fluctuating quasimolecule is somehow ambiguous, especially when the molecular lifetime is very short. As a result, fluctuating *metastable* preformed pairs would not give an exponential temperature dependence of S . However, as mentioned previously, the growth of low-energy pairing fluctuations or *metastable* preformed pairs with nearly zero center of mass momentum near T_c decreases the entropy S . In addition, because this growth is more remarkable at lower temperatures near T_c , the entropy S becomes a *convex* function of temperature, so that Eq. (13) gives the quite opposite temperature dependence of C_V to the case slightly in the BEC regime [$(k_F a_s)^{-1} \gtrsim 0.3$] near T_c .

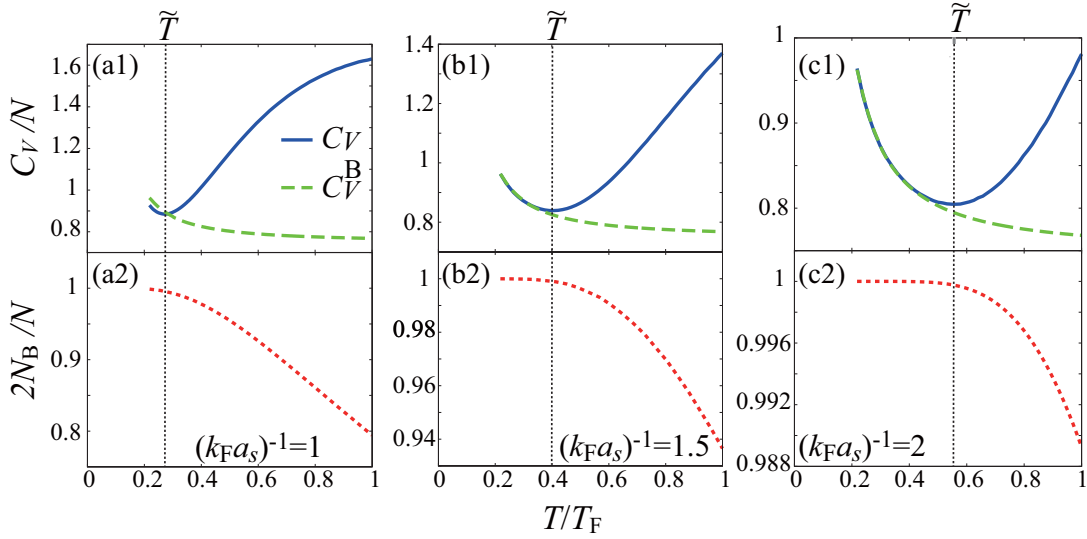


FIG. 5. (a1)–(c1) Specific heat $C_V(T \geq T_c)$ in the strong-coupling BEC regime [$(k_F a_s)^{-1} \geq 1$]. C_V^B is the specific heat in an ideal gas of $N/2$ bosons with a molecular mass $M = 2m$. (a2)–(c2) The number N_B of stable pairs. The characteristic temperature \tilde{T} is given as the temperature at which C_V takes a minimal value in the BEC regime.

The above-mentioned difference can also be understood for the viewpoint of the internal energy E . In the unitary regime, while the molecular picture is ambiguous, pairing fluctuations are known to induce particle-hole coupling [26], leading to a pseudogap structure around the Fermi level. This phenomenon would lower the internal energy E (as in the case of the ordinary BCS state), which would become more remarkable at lower temperature near T_c because of the enhancement of pairing fluctuations. As a result, E becomes a convex function of temperature, so that Eq. (7) gives the anomalous amplification of C_V in the unitary regime near T_c . On the other hand, slightly in the BEC regime where low-energy single-particle Fermi excitations near T_c are dominated by thermal dissociation of long-lived stable molecules, the internal energy would have an exponential-like temperature dependence, so that Eq. (7) gives the increase of C_V with increasing of the temperature near T_c .

Deep inside the BEC regime [$(k_F a_s)^{-1} \gtrsim 0.7$], we see in Figs. 5(a1)–5(c1) that the enhancement of C_V is revived near T_c , although it is not so remarkable as the case of unitary regime. In the temperature region where C_V increases with decreasing of the temperature, Figs. 5(a2)–5(c2) show that the system is dominated by long-lived *stable* pairs ($N_B \simeq N/2$). In addition, C_V in this temperature region is well described by the specific heat C_V^B of an ideal Bose gas with $N/2$ molecules, as shown in Figs. 5(a1)–5(c1). Thus, when one conveniently introduces the characteristic temperature \tilde{T} as the temperature at which $C_V(T)$ takes a minimum value, the region $T_c \leq T \lesssim \tilde{T}$ may be regarded as an almost ideal Bose gas of long-lived stable molecules.

We briefly note that such a Bose gas behavior of C_V can also be confirmed analytically. In the strong coupling BEC regime, the particle-particle scattering matrix $\Gamma(\mathbf{q}, i\nu_n)$ in Eq. (5) is reduced to [39]

$$\Gamma(\mathbf{q}, i\nu_n) = \frac{8\pi}{m^2 a_s} \frac{1}{i\nu_n - \frac{q^2}{4m} + \mu_B}, \quad (16)$$

where $\mu_B = 2\mu + E_{\text{bind}}^{2b}$. In obtaining Eq. (16), we have used the well-known result in the BEC regime, $\mu \simeq -E_{\text{bind}}^{2b}/2 = -1/(2ma_s^2) \ll -\epsilon_F$ [3–5]. Substituting Eq. (16) into the internal energy in Eq. (8), one has

$$E = \sum_{\mathbf{q}} \frac{q^2}{4m} n_B \left(\frac{q^2}{4m} - \mu_B \right) - E_{\text{bind}} \frac{N}{2}. \quad (17)$$

Here, we have assumed that all the Fermi atoms form tightly bound molecules, for simplicity. Since the specific heat $C_V = (\partial E / \partial T)_{V, N}$ is simply obtained from the first term in Eq. (17), it is just the same as the specific heat in an ideal gas with $N/2$ two-body bound molecules.

With increasing temperature above \tilde{T} , the gradual decrease of the number N_B of stable pairs from $N/2$, as shown in Figs. 5(a2)–5(c2), indicates the thermal dissociation of molecules. As shown in Eq. (15), this phenomenon naturally increases C_V , giving the deviation from C_V^B seen in Figs. 5(a1)–5(c1).

Plotting \tilde{T} in the phase diagram of an ultracold Fermi gas in terms of the interaction strength and the temperature, we obtain Fig. 6. As discussed above, this line physically gives the boundary between the region (NB) of an almost ideal Bose gas with $N/2$ noncondensed long-lived stable pairs and the so-called pseudogap regime (PG), where metastable preformed pairs dominate over the system. Particularly at T_c , this boundary is at $(k_F a_s)^{-1} \simeq 0.8$. We briefly point out that this value is consistent with the previous result $(k_F a_s)^{-1} \simeq 0.75$ [39], which was determined from the analyses of Fermi single-particle excitations.

We note that the boundary between the pseudogap regime (PG) and the normal Bose gas regime (NB) has previously been given by $T' = 2|\mu|$ (where $\mu < 0$) [24,26]. The background idea for this characteristic temperature is that $2|\mu|$ eventually coincides with the binding energy $E_{\text{bind}}^{2b} = 1/(ma_s^2)$ of a two-body bound molecule in the BEC limit, so that stable molecules are expected to appear below $T' \sim E_{\text{bind}}^{2b}$, overwhelming

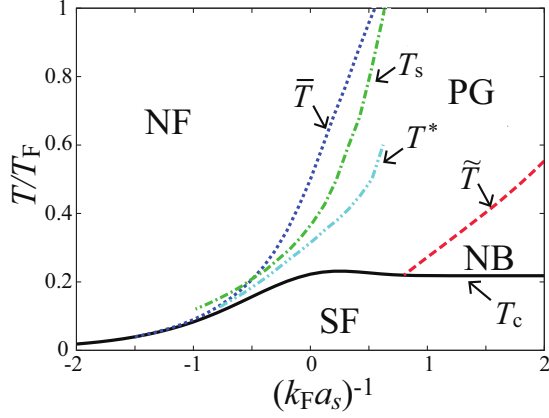


FIG. 6. Phase diagram of an ultracold Fermi gas with respect to the interaction strength $(k_F a_s)^{-1}$ and the temperature T , scaled by the Fermi temperature T_F . The characteristic temperature \tilde{T} gives the boundary between the region (NB) of an almost ideal Bose gas with $N/2$ noncondensed long-lived stable pairs and the pseudogap regime (PG), where the system is dominated by metastable preformed Cooper pairs or pairing fluctuations. \tilde{T} physically gives the boundary between the normal Fermi gas regime (NF) and PG. The region below T_c is in the superfluid state. For comparison, we also plot the previous pseudogap temperature T^* [24] obtained from the density of states $\rho(\omega)$, as well as the spin-gap temperature T_s [29] determined from the spin susceptibility χ_s . We note that T_c is only the phase transition temperature. \tilde{T} , \bar{T} , and T^* , as well as T_s , are all characteristic temperatures without being accompanied by any phase transition.

thermal dissociation. However, comparing T' with \tilde{T} , one finds that they are actually very different, as $T' \gg \tilde{T}$ (although we do not explicitly show this comparison here). This indicates that, although stable pairs would start to appear around $T' \sim E_{\text{bind}}^{2b}$, it does not immediately mean the realization of a molecular Bose gas. To obtain a gas of long-lived stable pairs, we need to further decrease the temperature down to \tilde{T} , at least for the viewpoint of the specific heat C_V . In this sense, the region between T' and \tilde{T} may be regarded as the crossover region between a gas of metastable quasimolecules and that of long-lived stable molecules.

We note that the physical meaning of \tilde{T} is different from the previous pseudogap temperature T^* [24] and the spin-gap temperature T_s [27,29], because the latter two physically give the boundary between the normal Fermi gas regime (NF) and PG. In this regard, we point out that the specific heat C_V can also give the other characteristic temperature, which we denote \bar{T} , corresponding to T^* and T_s . As seen in Fig. 7, when one moves to the weak-coupling BCS side $[(k_F a_s)^{-1} \lesssim 0]$ from the unitary regime, the enhancement of C_V near T_c (which is caused by metastable preformed pairs) gradually disappears, and the temperature dependence of C_V is reduced to that in a free Fermi gas, given by

$$C_V^F = 2 \sum_p \varepsilon_p \frac{\partial f(\xi_p)}{\partial T}. \quad (18)$$

Equation (18) is proportional to T when $T \ll T_F$ [see Eq. (11)]. It approaches the classical Dulong-Petit law $C_V^{\text{cl}} = 3N/2$ [57] in the high temperature region. Thus, the temperature ($\equiv \bar{T}$) at

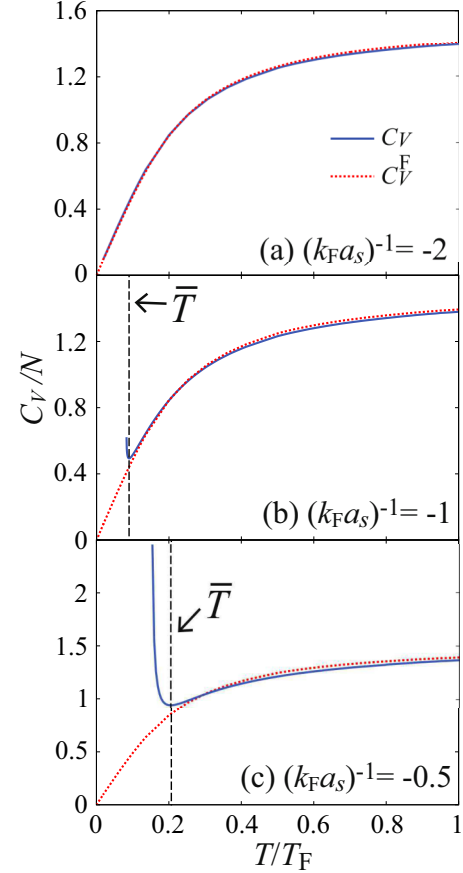


FIG. 7. Calculated specific heat C_V in the BCS side $[(k_F a_s)^{-1} \leq 0]$ as a function of temperature T , scaled by the Fermi temperature T_F . C_V^F is the specific heat in a free Fermi gas in Eq. (18). The characteristic temperature \bar{T} is determined as the temperature at which C_V becomes minimal.

which C_V takes a minimal value in Fig. 7 may be reasonably interpreted as the boundary between the normal Fermi gas regime (NF) and the pseudogap gap regime (PG) dominated by fluctuating metastable preformed Cooper pairs. Indeed, when we plot this characteristic temperature \bar{T} in Fig. 6, it is found to be consistent with T^* and T_s , as expected.

Finally, we compare our result with the recent experiment on a ${}^6\text{Li}$ unitary Fermi gas [41]. Figure 8 shows that our result well explains the observed amplification of C_V near T_c , indicating that the observed anomaly is due to *metastable* preformed Cooper pairs. However, Fig. 8 also shows that our result overestimates this enhancement near T_c . In this regard, we recall that a finite spacial resolution inherent in this experiment in a trapped geometry could lead to a possible suppression of the specific heat near T_c [41]. We also point out that, since we deal with pairing fluctuations within the simplest NSR level, inclusion of higher-order strong-coupling corrections beyond this approximation may also be important to correctly describe the behavior of the specific heat C_V , especially near T_c . Thus, we need further analyses to quantitatively explain this experimental result.

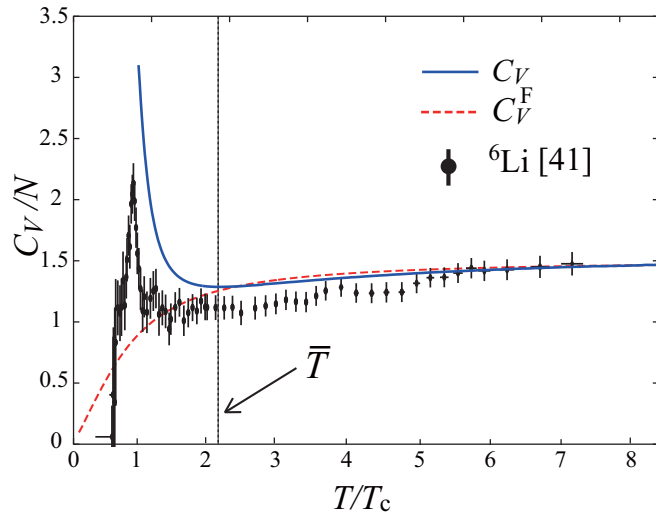


FIG. 8. Comparison of our result with the recent experiment on a ${}^6\text{Li}$ unitary Fermi gas [41]. In this figure, the temperature is normalized by T_c . C_V^F is the specific heat in a free Fermi gas.

IV. SUMMARY

To summarize, we have discussed the specific heat at constant volume C_V in the BCS-BEC-crossover regime of an ultracold Fermi gas. Including pairing fluctuations within the framework of the strong-coupling theory developed by Nozières and Schmitt-Rink, we clarified the temperature dependence of this thermodynamic quantity over the entire BCS-BEC-crossover region above T_c . In the unitary regime, we found that the specific heat is anomalously amplified near T_c , which is due to the appearance of fluctuating *metastable* preformed Cooper pairs. Although this anomaly disappears as soon as one goes to the BEC side, C_V was found to be again enhanced near T_c with further increasing of the interaction strength. We showed that this regime is dominated by long-lived *stable* pairs, and the enhancement of C_V in this region agrees well with the case of an ideal molecular Bose gas.

Using these results, we determined the characteristic temperature \tilde{T} , which physically distinguishes between the pseudogap regime where the system is dominated by metastable preformed Cooper pairs (or pairing fluctuations) and the region of an almost ideal Bose gas with $N/2$ noncondensed stable pairs. From the temperature dependence of the specific heat in the BCS side, we also determined the other characteristic temperature \bar{T} , which physically distinguishes between the normal Fermi gas regime and the pseudogap regime. Using \tilde{T} and \bar{T} , as well as the superfluid phase transition temperature T_c , we obtained the phase diagram of an ultracold Fermi gas in terms of the interaction strength and the temperature, consisting of (1) the normal Fermi gas regime, (2) the pseudogap regime dominated by metastable preformed Cooper pairs or pairing fluctuations, (3) the region of an almost ideal Bose gas with $N/2$ noncondensed long-lived stable pairs, and (4) the superfluid phase below T_c . Although \tilde{T} and \bar{T} are not accompanied by any phase transition, they are still useful in considering the strong-coupling properties of an ultracold Fermi gas in the BCS-BEC-crossover region.

We note that, although the background physics of \bar{T} is similar to that of the previous pseudogap temperature T^* , which is determined from the density of states $\rho(\omega)$, as well as that of the spin-gap temperature T_s , which is determined from the spin susceptibility χ_s , it is difficult to obtain the characteristic temperature corresponding to \bar{T} from $\rho(\omega)$ and χ_s . This is because they almost vanish in the strong-coupling BEC regime, due to the formation of tightly bound spin-singlet pairs with a large binding energy. In contrast, the specific heat is not suppressed in the BEC regime, so that we can safely determine \bar{T} to identify the region consisting of stable pairs below \bar{T} . In addition, the specific heat is known to exhibit singularity at T_c . These advantages indicate that the specific heat is a useful quantity in constructing the phase diagram of an ultracold Fermi gas in the BCS-BEC-crossover region.

We note that we have included strong-coupling corrections within the simplest NSR theory in this paper. In this regard, while the NSR theory can describe the BCS-BEC-crossover behavior of T_c , this strong-coupling theory is known to overestimate the pseudogap phenomenon associated with pairing fluctuations [24,27]. Since the NSR specific heat at the unitarity overestimates the observed enhancement of C_V near T_c in a ${}^6\text{Li}$ Fermi gas (see Fig. 8), a more sophisticated treatment of pairing fluctuations beyond the NSR theory would be necessary in order to quantitatively explain this experiment. In addition, since the NSR theory completely ignores an effective interaction between molecular bosons [61,62], it is also a crucial issue to clarify to what extent this molecular interaction affects the characteristic temperature \tilde{T} (which physically gives the boundary between the region of (long-lived) stable molecules and the region of metastable preformed pairs). For this problem, the so-called self-consistent T -matrix approximation [21] would be useful.

We also note that we have only dealt with the normal state above T_c in this paper. Thus, extension of the present theory to the superfluid phase below T_c is also an interesting challenge. In addition, we have ignored effects of a harmonic trap in this paper. Although these effects should in principle be unimportant regarding the fact that the recent experimental result shown in Fig. 8 represents that of a uniform Fermi gas, it has been pointed by the authors of this experiment [41] that the trap geometry may induce an error in the temperature measurement. To quantitatively compare our result with the experiment data, we need to theoretically include this point. Although the pseudogap phenomenon associated with pairing fluctuations has recently attracted much attention in cold Fermi gas physics, the pseudogap temperature between the normal Fermi gas regime and the pseudogap regime has so far been mainly discussed. Thus, our results would contribute to the further understanding of BCS-BEC-crossover physics in an ultracold Fermi gas on the viewpoint of the preformed pairs.

ACKNOWLEDGMENTS

We would like to thank D. Inotani and M. Matsumoto for useful discussions. This work was supported by KiPAS project in Keio University. R.H. and H.T. were supported by a Grant-in-Aid for JSPS fellows. Y.O. was also supported by a Grant-in-Aid for Scientific Research from MEXT and JSPS in Japan (Grants No. 25400418 and No. 15H00840).

APPENDIX: EXPRESSION FOR THE NUMBER N_B OF STABLE MOLECULES

To extract the contribution of stable molecules from the NSR term N_{NSR} in Eq. (9), it is convenient to write it in the spectral representation as

$$N_{\text{NSR}} = 2 \int_{-\infty}^{\infty} d\omega n_B(\omega) \rho_B(\omega). \quad (\text{A1})$$

Here, $\rho_B(\omega) = \sum_{\mathbf{q}} A_B(\mathbf{q}, \omega)$ may be viewed as the molecular density of states, and the factor two means that each molecule consists of two Fermi atoms. The molecular spectral weight $A_B(\omega)$ in $\rho_B(\omega)$ has the form

$$A_B(\mathbf{q}, \omega) = -\frac{1}{\pi} \text{Im} \left[\Gamma(\mathbf{q}, \omega_+) \frac{\partial}{\partial(2\mu)} \Pi(\mathbf{q}, \omega_+) \right]. \quad (\text{A2})$$

In Eq. (A2), we have used the simplified notations, $\Gamma(\mathbf{q}, \omega_+) = \Gamma(\mathbf{q}, i\nu_n \rightarrow \omega + i\delta)$ and $\Pi(\mathbf{q}, \omega_+) = \Pi(\mathbf{q}, i\nu_n \rightarrow \omega + i\delta)$, where δ is an infinitesimally small positive number.

When the analytic continued particle-particle scattering matrix $\Gamma(\mathbf{q}, \omega_+)$ has a real pole at $\omega = \omega_q$, it can be approximated to

$$\begin{aligned} \Gamma(\mathbf{q}, \omega_+) &= \frac{1}{\frac{m}{4\pi a_s} + \Pi(\mathbf{q}, \omega_+) - \sum_p \frac{1}{2\varepsilon_p}} \\ &\simeq \frac{1}{[\omega_+ - \omega_q] \frac{\partial}{\partial\omega_q} \Pi(\mathbf{q}, \omega_q)}. \end{aligned} \quad (\text{A3})$$

The contribution of the pole at $\omega = \omega_q$ to the number equation is evaluated by substituting Eq. (A3) into Eq. (A2). Since the real pole ω_q physically describes the dispersion of a stable molecule,

$$N_B = \sum_{\mathbf{q}:\text{pole}} n_B(\omega_q) \frac{\frac{\partial}{\partial(2\mu)} \Pi(\mathbf{q}, \omega_q)}{\frac{\partial}{\partial\omega_q} \Pi(\mathbf{q}, \omega_q)} \quad (\text{A4})$$

has the meaning of the number of stable pairs, where the summation is taken over real poles of $\Gamma(\mathbf{q}, \omega_+)$.

The contribution N_{sc} of scattering states to the number N of Fermi atoms is then given by

$$N_{\text{sc}} = N_{\text{NSR}} - 2N_B. \quad (\text{A5})$$

-
- [1] D. M. Eagles, *Phys. Rev.* **186**, 456 (1969).
[2] A. J. Leggett, in *Modern Trends in the Theory of Condensed Matter* (Springer, Berlin, 1960).
[3] P. Nozières and S. Schmitt-Rink, *J. Low Temp. Phys.* **59**, 195 (1985).
[4] C. A. R. Sa de Melo, M. Randeria, and J. R. Engelbrecht, *Phys. Rev. Lett.* **71**, 3202 (1993).
[5] M. Randeria, in *Bose-Einstein Condensation*, edited by A. Griffin, D. W. Snoke, and S. Stringari (Cambridge University Press, New York, 1995), p. 355.
[6] Y. Ohashi and A. Griffin, *Phys. Rev. Lett.* **89**, 130402 (2002).
[7] A. Perali, P. Pieri, G. C. Strinati, and C. Castellani, *Phys. Rev. B* **66**, 024510 (2002).
[8] S. Giorgini, S. Pitaevskii, and S. Stringari, *Rev. Mod. Phys.* **80**, 1215 (2008).
[9] I. Bloch, J. Dalibard, and W. Zwerger, *Rev. Mod. Phys.* **80**, 885 (2008).
[10] Q. J. Chen, J. Stajic, S. N. Tan, and K. Levin, *Phys. Rep.* **412**, 1 (2005).
[11] W. Ketterle and M. W. Zwierlein, in *Ultracold Fermi Gases*, edited by M. Inguscio, W. Ketterle, and C. Salomon (IOS Press, Amsterdam, 2008).
[12] C. A. Regal, M. Greiner, and D. S. Jin, *Phys. Rev. Lett.* **92**, 040403 (2004).
[13] M. W. Zwierlein, C. A. Stan, C. H. Schunck, S. M. F. Raupach, A. J. Kerman, and W. Ketterle, *Phys. Rev. Lett.* **92**, 120403 (2004).
[14] J. Kinast, S. L. Hemmer, M. E. Gehm, A. Turlapov, and J. E. Thomas, *Phys. Rev. Lett.* **92**, 150402 (2004).
[15] M. Bartenstein, A. Altmeyer, S. Riedl, S. Jochim, C. Chin, J. H. Denschlag, and R. Grimm, *Phys. Rev. Lett.* **92**, 203201 (2004).
[16] E. Timmermans, K. Furuya, P. W. Milonni, and A. K. Kerman, *Phys. Lett. A* **285**, 228 (2001).
[17] M. Holland, S. J. J. M. F. Kokkelmans, M. L. Chiofalo, and R. Walser, *Phys. Rev. Lett.* **87**, 120406 (2001).
[18] C. Chin, R. Grimm, P. Julienne, and E. Tiesinga, *Rev. Mod. Phys.* **82**, 1225 (2010).
[19] Y. Ohashi and A. Griffin, *Phys. Rev. A* **67**, 063612 (2003).
[20] H. Hu, X. J. Liu, and P. D. Drummond, *Phys. Rev. A* **73**, 023617 (2006).
[21] R. Haussmann, W. Rantner, S. Cerrito, and W. Zwerger, *Phys. Rev. A* **75**, 023610 (2007).
[22] N. Fukushima, Y. Ohashi, E. Taylor, and A. Griffin, *Phys. Rev. A* **75**, 033609 (2007).
[23] H. Hu, X. J. Liu, and P. D. Drummond, *Phys. Rev. A* **77**, 061605 (2008).
[24] S. Tsuchiya, R. Watanabe, and Y. Ohashi, *Phys. Rev. A* **80**, 033613 (2009).
[25] Q. Chen and K. Levin, *Phys. Rev. Lett.* **102**, 190402 (2009).
[26] S. Tsuchiya, R. Watanabe, and Y. Ohashi, *Phys. Rev. A* **84**, 043647 (2011).
[27] T. Kashimura, R. Watanabe, and Y. Ohashi, *Phys. Rev. A* **86**, 043622 (2012).
[28] G. Wlazlowski, P. Magierski, J. E. Drut, A. Bulgac, and K. J. Roche, *Phys. Rev. Lett.* **110**, 090401 (2013).
[29] H. Tajima, T. Kashimura, R. Hanai, R. Watanabe, and Y. Ohashi, *Phys. Rev. A* **89**, 033617 (2014).
[30] C. Chin, M. Bartenstein, A. Altmeyer, S. Riedl, S. Jochim, J. Hecker Denschlag, and R. Grimm, *Science* **305**, 1128 (2004).
[31] M. W. Zwierlein, J. R. Abo-Shaer, A. Schirotzek, C. H. Schunck, and W. Ketterle, *Nature (London)* **435**, 1051 (2005).
[32] J. Kinast, A. Turlapov, J. E. Thomas, Q. Chen, J. Stajic, and K. Levin, *Science* **307**, 1296 (2005).

- [33] A. Altmeyer, S. Riedl, C. Kohstall, M. J. Wright, R. Geursen, M. Bartenstein, C. Chin, J. H. Denschlag, and R. Grimm, *Phys. Rev. Lett.* **98**, 040401 (2007).
- [34] J. T. Stewart, J. P. Gaebler, and D. S. Jin, *Nature (London)* **454**, 744 (2008).
- [35] L. Luo and J. E. Thomas, *J. Low Temp. Phys.* **154**, 1 (2009).
- [36] J. P. Gaebler, J. T. Stewart, T. E. Drake, D. S. Jin, A. Perali, P. Pieri, and G. C. Strinati, *Nat. Phys.* **6**, 569 (2010).
- [37] M. Horikoshi, S. Nakajima, M. Ueda, and T. Mukaiyama, *Science* **327**, 442 (2010).
- [38] S. Nascimbene, N. Navon, K. J. Jiang, F. Chevy, and C. Salomon, *Nature (London)* **463**, 1057 (2010).
- [39] A. Perali, F. Palestini, P. Pieri, G. C. Strinati, J. T. Stewart, J. P. Gaebler, T. E. Drake, and D. S. Jin, *Phys. Rev. Lett.* **106**, 060402 (2011).
- [40] C. Sanner, E. J. Su, A. Keshet, W. Huang, J. Gillen, R. Gommers, and W. Ketterle, *Phys. Rev. Lett.* **106**, 010402 (2011).
- [41] M. J. H. Ku, A. T. Sommer, L. W. Cheuk, and M. W. Zwierlein, *Science* **335**, 563 (2012).
- [42] Y. Sagi, T. E. Drake, R. Paudel, R. Chapurin, and D. S. Jin, *Phys. Rev. Lett.* **114**, 075301 (2015).
- [43] A. Perali, C. Castellani, C. Di Castro, M. Grilli, E. Piegari, and A. A. Varlamov, *Phys. Rev. B* **62**, R9295 (2000).
- [44] S. Kasahara, T. Watashige, T. Hanaguri, Y. Kohsaka, T. Yamashita, Y. Shimoyama, Y. Mizukami, R. Endo, H. Ikeda, K. Aoyama, T. Terashima, S. Uji, T. Wolf, H. von Lohneysen, T. Shibauchi, and Y. Matsuda, *Proc. Natl. Acad. Sci. USA* **111**, 16309 (2014).
- [45] Y. Yanase and K. Yamada, *J. Phys. Soc. Jpn.* **70**, 1659 (2001).
- [46] A. Damascelli, Z. Hussain, and Z.-X. Shen, *Rev. Mod. Phys.* **75**, 473 (2003).
- [47] P. Lee, N. Nagaosa, and X. Wen, *Rev. Mod. Phys.* **78**, 17 (2006).
- [48] Ch. Renner, B. Revaz, J.-Y. Genoud, K. Kadowaki, and O. Fischer, *Phys. Rev. Lett.* **80**, 149 (1998).
- [49] K. Tanaka, W. S. Lee, D. H. Lu, A. Fujimori, T. Fujii, Risdiana, I. Terasaki, D. J. Scalapino, T. P. Devereaux, Z. Hussain, and Z.-X. Shen, *Science* **314**, 1910 (2006).
- [50] D. Pines, *Z. Phys. B* **103**, 129 (1996).
- [51] A. Kampf and J. R. Schrieffer, *Phys. Rev. B* **41**, 6399 (1990).
- [52] S. Chakravarty, R. B. Laughlin, D. K. Morr, and C. Nayak, *Phys. Rev. B* **63**, 094503 (2001).
- [53] B. L. Altshuler, L. B. Ioffe, and A. J. Millis, *Phys. Rev. B* **53**, 415 (1996).
- [54] Y. Yoshinari, H. Yasuoka, Y. Ueda, K. Koga, and K. Kosuge, *J. Phys. Soc. Jpn.* **59**, 3698 (1990).
- [55] G. Zheng, T. Odaguchi, T. Mito, Y. Kitaoka, K. Asayama, and Y. Kodama, *J. Phys. Soc. Jpn.* **62**, 2591 (1993).
- [56] D. J. Thouless, *Ann. Phys.* **10**, 553 (1960).
- [57] A. L. Fetter and J. D. Walecka, *Quantum Theory of Many-Particle Systems* (Dover Publications, New York, 2003).
- [58] N. E. Phillips, *Phys. Rev.* **114**, 676 (1959).
- [59] J. R. Engelbrecht, Ph.D. thesis, University of Illinois at Urbana Champaign, 1993.
- [60] We see in Fig. 2(b) that N_{sc} is slightly negative when $(k_F a_s)^{-1} \gtrsim 0.3$. This is because all the scattering states cannot actually be simply described by quasimolecules with a finite lifetime [6,59].
- [61] P. Pieri and G. C. Strinati, *Phys. Rev. B* **61**, 15370 (2000).
- [62] D. S. Petrov, C. Salomon, and G. V. Shlyapnikov, *Phys. Rev. Lett.* **93**, 090404 (2004).